

$\phi \rightarrow \pi^0 \eta \gamma$  and  $\phi \rightarrow \pi^0 \pi^0 \gamma$  decays and mixing between low and high mass scalar mesons

T. Teshima,\* I. Kitamura, and N. Morisita

*Department of Natural Sciences, Chubu University, Kasugai 487-8501, Japan*

(Received 19 March 2007; revised manuscript received 25 June 2007; published 12 September 2007)

Radiative decays  $\phi \rightarrow \eta \pi^0 \gamma$  and  $\phi \rightarrow \pi^0 \pi^0 \gamma$  are studied assuming that these decays are caused through the intermediate  $a_0(980)\gamma$  and  $f_0(980)\gamma$  states, respectively. Fitting the experimental data of the  $\eta \pi^0$  and  $\pi^0 \pi^0$  invariant mass spectrum in the decays  $\phi \rightarrow \eta \pi^0 \gamma$  and  $\pi^0 \pi^0 \gamma$ , it is shown that the processes  $\phi \rightarrow a_0 \gamma$  and  $\phi \rightarrow f_0 \gamma$  are dominated by the  $K^+ K^-$  loop interaction rather than the pointlike  $\phi a_0(f_0)\gamma$  one both for the nonderivative and derivative *SPP* coupling. The experimental data of  $\Gamma[\phi \rightarrow f_0 \gamma]/\Gamma[\phi \rightarrow a_0 \gamma]$  predicts that  $g_{f_0 K \bar{K}}/g_{a_0 K \bar{K}} \sim 2$ . Considering the effects of the mixing between low mass scalar  $q\bar{q}\bar{q}$  states and high mass scalar  $q\bar{q}$  states to these coupling constants  $g_{f_0 K \bar{K}}$  and  $g_{a_0 K \bar{K}}$ , one suggests that this mixing is rather large.

DOI: 10.1103/PhysRevD.76.054002

PACS numbers: 12.39.Mk, 12.40.Yx, 13.66.Jn

## I. INTRODUCTION

For a long time, the radiative decays of the  $\phi$  to  $\pi^0 \eta \gamma$  and  $\pi^0 \pi^0 \gamma$  have been analyzed, assuming that the decays  $\phi \rightarrow \pi^0 \eta (\pi^0) \gamma$  proceed through the  $\phi \rightarrow a_0(f_0)\gamma$  decays, to reveal the structure of the light scalar mesons  $a_0(980)$  and  $f_0(980)$  [1–3]. These analyses are performed assuming the charged  $K^+ K^-$  loop diagram in the coupling  $\phi a_0(f_0)\gamma$  and the pointlike (vector dominance)  $\phi a_0(f_0)\gamma$  interaction. In this work, we analyze the data for the  $\pi^0 \eta$  and  $\pi^0 \pi^0$  invariant mass spectrum in  $\phi \rightarrow \pi^0 \eta \gamma$  and  $\phi \rightarrow \pi^0 \pi^0 \gamma$  decays given in a recent precise experiment [4], assuming charged  $K^+ K^-$  loop diagram and pointlike  $\phi f_0(a_0)\gamma$  interaction. For the *S* (scalar meson)-*P* (pseudoscalar meson)-*P* (pseudoscalar meson) interactions appeared in these decaying processes, we consider the cases a nonderivative interaction and a derivative one, the latter of which is adopted in the literature [3]. The result obtained in our present analysis shows that these processes are caused through the  $K^+ K^-$  loop diagram dominantly.

When the  $K^+ K^-$  loop diagram is dominant in the decays  $\phi \rightarrow f_0 \gamma \rightarrow \pi^0 \pi^0 \gamma$  and  $\phi \rightarrow a_0 \gamma \rightarrow \pi^0 \eta \gamma$ , the value of the ratio  $g_{f_0 K \bar{K}}/g_{a_0 K \bar{K}}$  is obtained from the experimental ratio  $\Gamma(\phi \rightarrow a_0 \gamma)/\Gamma(\phi \rightarrow f_0 \gamma)$ , that is the rather large value  $g_{f_0 K \bar{K}}/g_{a_0 K \bar{K}} \sim 2$ . These coupling constant strengths depend on the structure of the scalar mesons, that is, these scalar mesons are constituted of  $q\bar{q}$  or  $qq\bar{q}\bar{q}$ , or are mixing states of  $q\bar{q}$  and  $qq\bar{q}\bar{q}$ . Many authors in Refs. [1–3] argue that the data of  $\phi \rightarrow a_0(f_0)\gamma \rightarrow \pi^0 \eta (\pi^0) \gamma$  decays gives evidence in favor of the  $qq\bar{q}\bar{q}$  nature for the scalar  $a_0(980)$  and  $f_0(980)$  mesons, and several authors in Refs. [1–3] argue the matter of mixing between  $q\bar{q}$  and  $qq\bar{q}\bar{q}$  states.

Much recent literature (refer to the “Note on scalar mesons” in [5]) suggests that the low mass scalar nonet ( $f_0(600)$ ,  $K_0^*(800)$ ,  $a_0(980)$ ,  $f_0(980)$ ) are the  $qq\bar{q}\bar{q}$  state

and the high mass scalar mesons ( $a_0(1450)$ ,  $K_0^*(1430)$ ,  $f_0(1370)$ ,  $f_0(1500)$ ,  $f_0(1710)$ ) are the conventional  $L = 1q\bar{q}$  nonet plus one glueball. We assume a strong mixing between low mass and high mass scalar mesons to explain the fact that the high  $L = 1q\bar{q}$  scalar nonet are so high compared to other  $L = 1q\bar{q}$   $1^{++}$  and  $2^{++}$  mesons [6,7]. Assuming that the coupling strengths causing the mixing between  $I = 1a_0(980)$  and  $a_0(1450)$ ,  $I = 1/2K_0^*(800)$  and  $K_0^*(1430)$ , and  $I = 0$  ( $f_0(600)$ ,  $f_0(980)$ ) and ( $f_0(1370)$ ,  $f_0(1500)$ ,  $f_0(1710)$ ) are the same, we analyzed the  $S \rightarrow PP$  decays using derivative *SPP* couplings [8]. Fitting the various experimental *SPP* decay widths, we obtained the mixing angle between  $a_0(980)$  and  $a_0(1450)$  as  $\sim 9^\circ$ . In our previous work [9], we analyzed the  $\Gamma(\phi \rightarrow f_0 \gamma)$  and  $\Gamma(\phi \rightarrow a_0 \gamma)$  assuming the pointlike (vector dominance) coupling for the  $a_0 \phi \gamma$  and  $f_0 \phi \gamma$  interaction and using the mixing strength obtained in previous work [8], and then suggested the importance of the mixing effect for the explanation of the rather large ratio  $\Gamma(\phi \rightarrow f_0 \gamma)/\Gamma(\phi \rightarrow a_0 \gamma)$ .

In Sec. II, we analyze the data for  $\pi^0 \eta$  and  $\pi^0 \pi^0$  invariant mass spectrum of the  $dBR(\phi \rightarrow \pi^0 \pi^0 \gamma)/dq$  and  $dBR(\phi \rightarrow \pi^0 \eta \gamma)/dq$  assuming the intermediate scalar states  $f_0(980)$  and  $a_0(980)$ . In this analysis, we consider the pointlike and  $K^+ K^-$  loop interaction for  $\phi f_0(a_0)\gamma$  coupling, in cases of the derivative and the nonderivative *SPP* coupling. In Sec. III, we reanalyze our mass formula for the low mass nonet scalar and the high mass nonet scalar + glueball adopting the new mass data of the  $K_0^*(800)$  [5]. In Sec. IV, we express the *SPP* coupling constants  $g_{a_0 \pi \pi}$ ,  $g_{f_0 \pi \pi}$ , etc. using the mixing parameters between low and high mass scalar mesons. We pursue the best-fit analysis for the  $S \rightarrow PP$  decay data using the mixing parameters obtained in Sec. III for both nonderivative and derivative *SPP* interactions, and then obtain the best-fit  $g_{f_0 K \bar{K}}$ , etc. Comparing the best fit  $g_{f_0 K \bar{K}}$ , etc. with the values obtained from the  $\phi \rightarrow f_0(a_0)\gamma$  decays, we suggest that the nonderivative coupling is more reasonable than the derivative one and the mixing between the  $q\bar{q}$  state and  $qq\bar{q}\bar{q}$  state is rather large.

\*teshima@isc.chubu.ac.jp

## II. ANALYSIS OF THE $\phi \rightarrow \pi^0 \eta \gamma$ AND $\phi \rightarrow \pi^0 \pi^0 \gamma$ DECAYS

### A. $\phi \rightarrow \pi^0 \eta \gamma$ decay

First, we consider the decay  $\phi \rightarrow a_0(980)\gamma \rightarrow \pi^0 \eta \gamma$  shown in Fig. 1. The invariant mass distribution of the branching ratio  $dBR(\phi \rightarrow a_0(980)\gamma \rightarrow \pi^0 \eta \gamma)/dm$  is expressed as (refer to the first paper in Ref. [1])

$$\frac{dBR(\phi \rightarrow a_0 \gamma \rightarrow \pi^0 \eta \gamma)}{dm} = \frac{2m^2}{\pi} \frac{1}{\Gamma_\phi} \frac{\Gamma(\phi \rightarrow a_0 \gamma; m) \Gamma(a_0 \rightarrow \pi^0 \eta; m)}{|D_{a_0}(m^2)|^2}, \quad (1)$$

where  $\Gamma_\phi$  is a decay width of  $\phi$  and  $1/D_{a_0}(m^2)$  represents the propagator of the intermediate state  $a_0$ ,

$$D_{a_0}(m^2) = m^2 - m_{a_0}^2 - im_{a_0} \Gamma_{a_0}. \quad (2)$$

$\Gamma(a_0 \rightarrow \pi^0 \eta; m)$  is the decay width on the virtual mass  $m$  of intermediate  $a_0$  defined as  $m = \sqrt{q_0^2 - \mathbf{q}^2}$ ,

$$\Gamma(a_0 \rightarrow \pi^0 \eta; m) = \frac{g_{a_0 \pi \eta}^2}{8\pi m^2} \frac{\sqrt{(m^2 - (m_\pi + m_\eta)^2)(m^2 - (m_\pi - m_\eta)^2)}}{2m} \times \begin{cases} 1 & \text{for nonderivative coupling,} \\ \frac{(m^2 - m_\pi^2 - m_\eta^2)^2}{2} & \text{for derivative coupling,} \end{cases} \quad (3)$$

where the coupling constant  $g_{a_0 \pi \eta}$  is defined as

$$M(a_0(q) \rightarrow \pi^0(q_1) + \eta(q_2)) = g_{a_0 \pi \eta} \times \begin{cases} 1 & \text{for nonderivative coupling,} \\ q_1 \cdot q_2 & \text{for derivative coupling.} \end{cases} \quad (4)$$

$\Gamma(\phi \rightarrow a_0 \gamma; m)$  is the decay width on the virtual mass  $m = \sqrt{q_0^2 - \mathbf{q}^2}$  of the intermediate state  $a_0$ ,

$$\Gamma(\phi \rightarrow a_0 \gamma; m) = \frac{\alpha}{3} g_{\phi a_0 \gamma}^2(m) \left( \frac{m_\phi^2 - m^2}{2m_\phi} \right)^3, \quad (5)$$

where the coupling constant  $g_{\phi a_0 \gamma}(m)$  is defined as

$$M(\phi(p, \epsilon_\phi) \rightarrow a_0(q) + \gamma(k, \epsilon_\gamma)) = e g_{\phi a_0 \gamma}(m) (p \cdot k \epsilon_\phi \cdot \epsilon_\gamma - p \cdot \epsilon_\gamma k \cdot \epsilon_\phi). \quad (6)$$

For the coupling  $g_{\phi a_0 \gamma}(m)$ , pointlike interaction and  $K^+ K^-$  loop interaction contribute as shown in Fig. 2, and then  $g_{\phi a_0 \gamma}(m)$  is expressed as

$$g_{\phi a_0 \gamma}(m) = g_{\phi a_0 \gamma}^{\text{pointlike}} + g_{\phi a_0 \gamma}^{K\bar{K} \text{ loop}}(m). \quad (7)$$

$g_{\phi a_0 \gamma}^{K\bar{K} \text{ loop}}(m)$  is calculated for nonderivative  $a_0 K^+ K^-$  coupling by many authors (N. N. Achasov *et al.* and F. E. Close

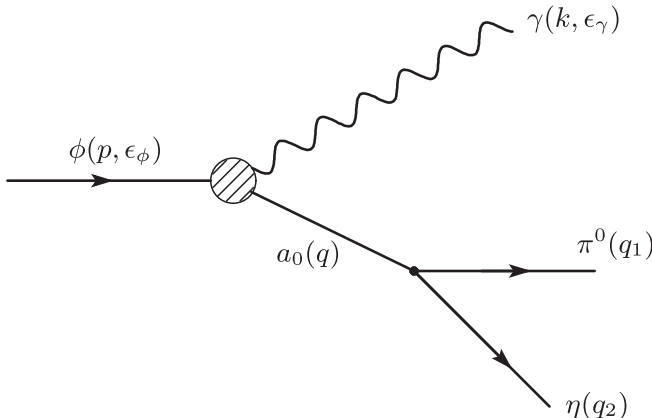


FIG. 1. Diagram for the decay  $\phi \rightarrow a_0(980)\gamma \rightarrow \pi^0 \eta \gamma$ .

*et al.* in [1]) considering three diagrams (a), (b), and (c) shown in Fig. 3, as

$$g_{\phi a_0 \gamma}^{K\bar{K} \text{ loop}}(m) = \frac{g_{\phi K\bar{K}} g_{a_0 K\bar{K}}}{2\pi^2 i m_K^2} I(a, b) \quad (8)$$

for nonderivative coupling.

The quantities  $a, b$  are defined as  $a = m_\phi^2/m_K^2$ ,  $b = m^2/m_K^2$  and  $I(a, b)$  arisen from the loop integral is

$$I(a, b) = \frac{1}{2(a-b)} - \frac{2}{(a-b)^2} \left\{ f\left(\frac{1}{b}\right) - f\left(\frac{1}{a}\right) \right\} + \frac{a}{(a-b)^2} \left\{ g\left(\frac{1}{b}\right) - g\left(\frac{1}{a}\right) \right\}, \quad (9)$$

where

$$f(x) = \begin{cases} -\left(\sin^{-1}\left(\frac{1}{2\sqrt{x}}\right)\right)^2, & x > \frac{1}{4} \\ \frac{1}{4} \left[ \log \frac{\eta_+}{\eta_-} - i\pi \right]^2, & x < \frac{1}{4} \end{cases},$$

$$g(x) = \begin{cases} \sqrt{4x-1} \sin^{-1}\left(\frac{1}{2\sqrt{x}}\right), & x > \frac{1}{4} \\ \frac{1}{2} \sqrt{1-4x} \left[ \log \frac{\eta_+}{\eta_-} - i\pi \right], & x < \frac{1}{4} \end{cases}, \quad (10)$$

$$\eta_\pm = \frac{1}{2x} (1 \pm \sqrt{1-4x}).$$

The coupling constant  $g_{\phi K\bar{K}}$  is defined as

$$M(\phi(p, \epsilon^\phi) \rightarrow K^+(q_1) + K^-(q_2)) = g_{\phi K\bar{K}} \epsilon_\mu^\phi (q_1^\mu - q_2^\mu), \quad (11)$$

and decay width is expressed as

$$\Gamma(\phi \rightarrow K^+ + K^-) = \frac{g_{\phi K\bar{K}}^2}{4\pi} \frac{2}{3m_\phi^2} \left( \frac{m_\phi^2}{4} - m_K^2 \right)^{3/2}. \quad (12)$$

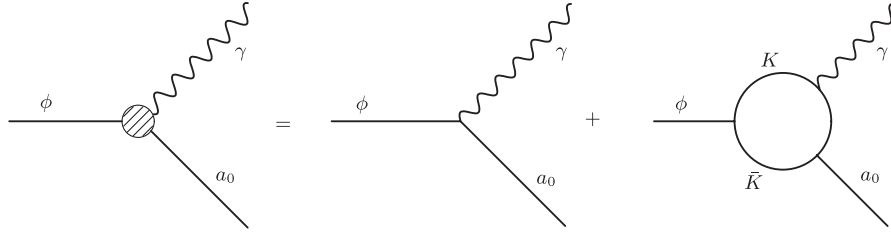


FIG. 2. Diagrams for the pointlike and  $K^+K^-$  loop coupling contributing to  $g_{\phi a_0 \gamma}(m)$ .

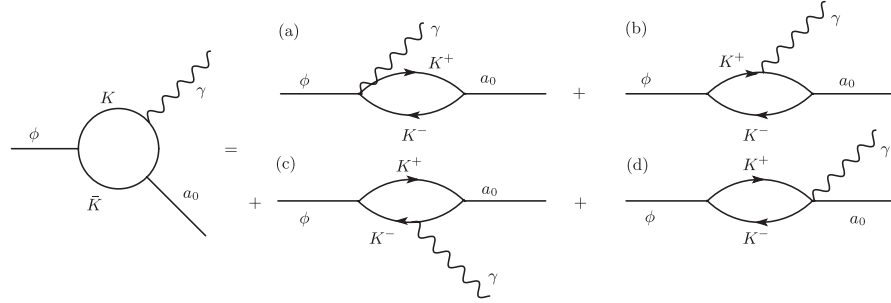


FIG. 3. Diagrams for the  $K^+K^-$  loop coupling contributing to  $g_{\phi a_0 \gamma}(m)$ .

The coupling constant  $g_{\phi K \bar{K}}$  is estimated using the experimental data  $\Gamma(\phi \rightarrow K^+ + K^-) = 2.10 \pm 0.05$  MeV [5] as

$$g_{\phi K \bar{K}} = 4.55 \pm 0.06. \quad (13)$$

For the  $a_0 K^+ K^-$  coupling,  $g_{a_0 K \bar{K}}$  is defined by the similar expression as Eq. (4)

$$M(a_0(q) \rightarrow K^+(q_1) + K^-(q_2)) = g_{a_0 K \bar{K}} \times \begin{cases} 1 & \text{for nonderivative coupling,} \\ q_1 \cdot q_2 & \text{for derivative coupling.} \end{cases} \quad (4')$$

For derivative coupling of the  $a_0 K^+ K^-$ ,  $K^+ K^-$  loop diagram contribution  $g_{\phi a_0 \gamma}^{K \bar{K} \text{ loop}}(m)$  is calculated by D. Black *et al.* [2] considering four diagrams (a), (b), (c), and (d) shown in Fig. 3, as

$$g_{\phi a_0 \gamma}^{K \bar{K} \text{ loop}}(m) = \frac{g_{\phi K \bar{K}} g_{a_0 K \bar{K}}}{2\pi^2 i m_K^2} \frac{2m_K^2 - m^2}{2} I(a, b) \quad (8')$$

for derivative coupling.

Using Eqs. (2), (3), (5), (7), (8), and (8'), we parametrize Eq. (1) as

$$\frac{dBR(\phi \rightarrow a_0 \gamma \rightarrow \pi^0 \eta \gamma)}{dm} = G_1 \frac{|G_2 + \frac{1}{i} [\frac{2m_K^2 - m^2}{2}] I(a, b)|^2}{|G_2 + \frac{1}{i} [\frac{2m_K^2 - m_a^2}{2}] I(a, b_0)|^2} \left( \frac{m_\phi^2 - m^2}{m_\phi^2 - m_a^2} \right)^3 \frac{m_a}{m} \frac{m_a^2 \Gamma_a^2}{(m^2 - m_a^2)^2 + m_a^2 \Gamma_a^2} \times \sqrt{\frac{(m^2 - (m_\eta + m_\pi)^2)(m^2 - (m_\eta - m_\pi)^2)}{(m_a^2 - (m_\eta + m_\pi)^2)(m_a^2 - (m_\eta - m_\pi)^2)}} \quad (14)$$

where  $G_1, G_2, b_0$  are defined as

$$G_1 = \frac{2}{\pi \Gamma_\phi \Gamma_a^2} \Gamma(\phi \rightarrow a_0 \gamma; m_a) \Gamma(a_0 \rightarrow \eta \pi^0; m_a), \quad (15)$$

$$G_2 = g_{\phi \gamma a}^{\text{pointlike}} / \left( \frac{g_{\phi K \bar{K}} g_{a_0 K \bar{K}}}{2\pi^2 m_K^2} \right), \quad b_0 = \frac{m_a^2}{m_K^2},$$

and factors  $[\frac{2m_K^2 - m^2}{2}]$  and  $[\frac{2m_K^2 - m_a^2}{2}]$  are replaced to 1 for nonderivative  $SPP$  coupling.  $\Gamma(a_0 \rightarrow \eta \pi^0, m_a)$  and

$\Gamma(\phi \rightarrow a_0 \gamma, m_a)$  are defined in Eqs. (3) and (5) setting  $m \rightarrow m_a$ . We fit the Eq. (14) varying the parameters  $G_1$  and  $G_2$  using the experimental data from the SND collaboration and KLEO collaboration in Ref. [4]. Best-fitted curves are shown in Fig. 4; the solid line for nonderivative  $SPP$  coupling and the dashed line for derivative  $SPP$  coupling are obtained for the choice of the parameters  $G_1$  and  $G_2$  as  $G_1 = 4.1 \times 10^{-4} \text{ GeV}^{-1}$ ,  $G_2 = -0.16$  for nonderivative coupling and  $G_1 = 3.9 \times 10^{-4} \text{ GeV}^{-1}$ ,  $G_2 = 0.08$  for derivative coupling. For these choices, the estimated

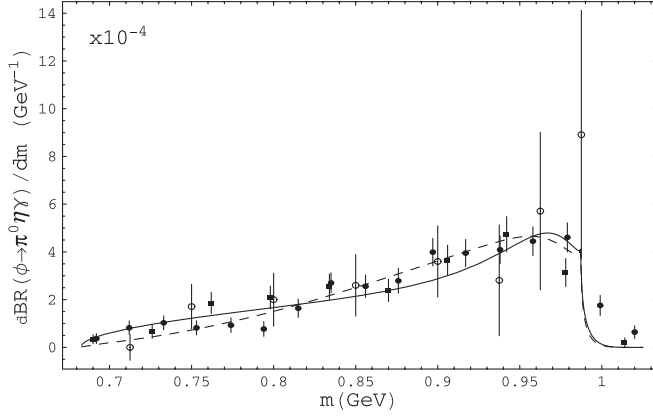


FIG. 4.  $dBR(\phi \rightarrow \pi^0 \eta \gamma)/dm$  (in unit of  $\text{GeV}^{-1}$ ) as a function of the  $\pi^0$ - $\eta$  invariant mass  $m$  (in  $\text{GeV}^{-1}$ ). The solid line shows the best-fitted curve for the nonderivative *SPP* coupling interaction and the dashed line shows the best-fitted curve for the derivative one. Experimental data indicated by circles are from the SND collaboration in Ref. [4], and those by filled circles and filled squares are from the KLEO collaboration in Ref. [4].

$BR(\phi \rightarrow \pi^0 \eta \gamma)$  are estimated as

$$\begin{aligned} G_1 &= 4.1 \times 10^{-4} \text{ GeV}^{-1}, \\ G_2 &= -0.16, \\ \chi^2/(\text{d.o.f}) &= 59.3/(35 - 1), \end{aligned} \quad (16)$$

$$\begin{aligned} BR(\phi \rightarrow \pi^0 \eta \gamma) &= 7.03 \times 10^{-5} \\ &\text{for nonderivative coupling,} \end{aligned}$$

$$\begin{aligned} G_1 &= 3.9 \times 10^{-4} \text{ GeV}^{-1}, \\ G_2 &= 0.08, \\ \chi^2/(\text{d.o.f}) &= 54.9/(35 - 1), \end{aligned} \quad (16')$$

$$\begin{aligned} BR(\phi \rightarrow \pi^0 \eta \gamma) &= 7.12 \times 10^{-5} \\ &\text{for derivative coupling.} \end{aligned}$$

The estimated value for  $BR(\phi \rightarrow \pi^0 \eta \gamma)$  is consistent with the experimental data  $BR^{\text{exp}}(\phi \rightarrow \pi^0 \eta \gamma) = (8.3 \pm$

$0.5) \times 10^{-5}$  [4,5]. Also, the estimated value of  $G_1$  is consistent with the value evaluated from the experimental data (Ref. [5]) using the relation Eq. (15),

$$\begin{aligned} G_1^{\text{exp}} &= \frac{2}{\pi \Gamma_a} BR^{\text{exp}}(\phi \rightarrow a_0 \gamma; m_a) BR^{\text{exp}}(a_0 \rightarrow \eta \pi^0; m_a) \\ &= (5.96 \pm 2.47) \times 10^{-4} \text{ GeV}^{-1}. \end{aligned}$$

Furthermore  $G_2$  is very small compared to  $|I(a, b_0)| = 0.902$  for  $m_a = 0.985 \text{ GeV}$ , then we can suppose that the  $K^+ K^-$  loop contribution is dominant in the  $\phi \rightarrow \pi^0 \eta \gamma$  decay. Supposing that the decay  $\phi \rightarrow a_0 \gamma$  is caused through only the  $K^+ K^-$  loop interaction, we obtain the result

$$\begin{aligned} \Gamma(\phi \rightarrow a_0 \gamma) &= \frac{\alpha}{3} \left| \frac{g_{\phi K \bar{K}} g_{a_0 K \bar{K}}}{2\pi^2 m_K^2} \left[ \frac{2m_K^2 - m_a^2}{2} \right] I(a, b_0) \right|^2 \\ &\quad \times \left( \frac{m_\phi^2 - m_a^2}{2m_\phi} \right)^3, \end{aligned} \quad (17)$$

where the factor  $\left[ \frac{2m_K^2 - m_a^2}{2} \right]$  is replaced to 1 for the non-derivative coupling. Using the value Eq. (13) of  $g_{\phi K \bar{K}}$  and the experimental value  $\Gamma(\phi \rightarrow a_0 \gamma) = (0.323 \pm 0.029) \times 10^{-3} \text{ MeV}$  in Ref. [5], we obtain the result

$$g_{a_0 K \bar{K}} = \begin{cases} 2.18 \pm 0.12 \text{ GeV}, & \text{for nonderivative coupling,} \\ 9.04 \pm 0.50 \text{ GeV}^{-1} & \text{for derivative coupling.} \end{cases} \quad (18)$$

Using relations Eqs. (3), (15), and (17) and estimated results Eqs. (16), (16'), and (18), we obtained the values for  $g_{a_0 \pi \eta}$ ,

$$g_{a_0 \pi \eta} = \begin{cases} 1.89 \pm 0.75 \text{ GeV}, & \text{for nonderivative coupling,} \\ 5.79 \pm 2.32 \text{ GeV}^{-1} & \text{for derivative coupling.} \end{cases} \quad (18')$$

## B. $\phi \rightarrow \pi^0 \pi^0 \gamma$ decay

For the decay  $\phi \rightarrow f_0 \gamma \rightarrow \pi^0 \pi^0 \gamma$ , the invariant mass distribution of the branching ratio  $dBR(\phi \rightarrow f_0 \gamma \rightarrow \pi^0 \pi^0 \gamma)/dm$  is expressed similar to Eq. (14) for the case  $\phi \rightarrow a_0 \gamma \rightarrow \pi^0 \eta \gamma$  as

$$\frac{dBR(\phi \rightarrow f_0 \gamma \rightarrow \pi^0 \pi^0 \gamma)}{dm} = G_1 \frac{|G_2 + \frac{1}{i} \left[ \frac{2m_K^2 - m^2}{2} \right] I(a, b)|^2}{|G_2 + \frac{1}{i} \left[ \frac{2m_K^2 - m^2}{2} \right] I(a, b_0)|^2} \left( \frac{m_\phi^2 - m^2}{m_\phi^2 - m_f^2} \right)^3 \frac{m_f}{m} \frac{m_f^2 \Gamma_f^2}{(m^2 - m_f^2)^2 + m_f^2 \Gamma_f^2} \sqrt{\frac{m^2 - 4m_\pi^2}{m_f^2 - 4m_\pi^2}}, \quad (19)$$

where  $G_1, G_2, b_0$  are defined as

$$G_1 = \frac{2}{\pi \Gamma_\phi \Gamma_f^2} \Gamma(\phi \rightarrow f_0 \gamma; m_f) \Gamma(f_0 \rightarrow \pi^0 \pi^0; m_f), \quad G_2 = g_{\phi \gamma f}^{\text{pointlike}} \left/ \left( \frac{g_{\phi K \bar{K}} g_{f_0 K \bar{K}}}{2\pi^2 m_K^2} \right) \right., \quad b_0 = \frac{m_f^2}{m_K^2}. \quad (20)$$

Here,  $\Gamma(f_0 \rightarrow \pi^0 \pi^0; m_f)$  and  $\Gamma(\phi \rightarrow f_0 \gamma; m_f)$  are expressed as

$\phi \rightarrow \pi^0 \eta \gamma$  AND ...

$$\begin{aligned} \Gamma(f_0 \rightarrow \pi^0 \pi^0 : m_f) &= \frac{g_{f_0 \pi \pi}^2}{16 \pi m_f^2} \frac{\sqrt{m_f^2 - 4m_\pi^2}}{2} \\ &\times \begin{cases} 1 & \text{for nonderivative coupling,} \\ \left(\frac{m_f^2 - 2m_\pi^2}{2}\right)^2 & \text{for derivative coupling,} \end{cases} \end{aligned} \quad (21)$$

where the coupling constant  $g_{f_0 \pi \pi}$  is defined as

$$\begin{aligned} M(f_0(q) \rightarrow \pi^0(q_1) + \pi^0(q_2)) &= \frac{1}{2} g_{f_0 \pi \pi} \\ &\times \begin{cases} 1 & \text{for nonderivative coupling,} \\ q_1 \cdot q_2 & \text{for derivative coupling,} \end{cases} \end{aligned} \quad (22)$$

and

$$\Gamma(\phi \rightarrow f_0 \gamma : m_f) = \frac{\alpha}{3} g_{\phi f_0 \gamma}^2 (m_f) \left( \frac{m_\phi^2 - m_f^2}{2m_\phi} \right)^3, \quad (23)$$

$$g_{\phi f_0 \gamma}(m_f) = g_{\phi f_0 \gamma}^{\text{pointlike}} + \frac{g_{\phi K \bar{K}} g_{f_0 K \bar{K}}}{2\pi^2 i m_K^2} \left[ \frac{2m_K^2 - m_f^2}{2} \right] I(a, b_0). \quad (24)$$

In Eq. (24), the factor  $\left[ \frac{2m_K^2 - m_f^2}{2} \right]$  is replaced to 1 for the nonderivative coupling.  $g_{f_0 K \bar{K}}$  is defined in the similar equation as Eq. (22),

$$\begin{aligned} M(f_0(q) \rightarrow K^+(q_1) + K^-(q_2)) &= g_{f_0 K \bar{K}} \\ &\times \begin{cases} 1 & \text{for nonderivative coupling,} \\ q_1 \cdot q_2 & \text{for derivative coupling.} \end{cases} \end{aligned} \quad (22')$$

We fit the Eq. (19) using the experimental data from the SND and KLEO collaborations in Ref. [4]. Many authors in Refs. [2] studied this process and obtained the result that the background process  $\phi \rightarrow \rho(+\sigma)\gamma \rightarrow \gamma\pi^0\pi^0$  is necessary to fit the low invariant mass region and the  $K^+K^-$  loop contribution is dominant in the high invariant mass region. In order to estimate the ratio of pointlike contribution  $G_2$  to the  $K^+K^-$  loop contribution  $G_1$ , we fit the Eq. (19) to high mass region data of  $m$  (0.6 GeV  $\sim$  1.0 GeV). The best-fit curves obtained are shown in Fig. 5; the solid line is for the nonderivative coupling and the dashed line is for the derivative one. The choice of the parameters  $G_1$  and  $G_2$  for these best-fit and estimated values for  $BR(\phi \rightarrow \pi^0 \pi^0 \gamma)$  are obtained as

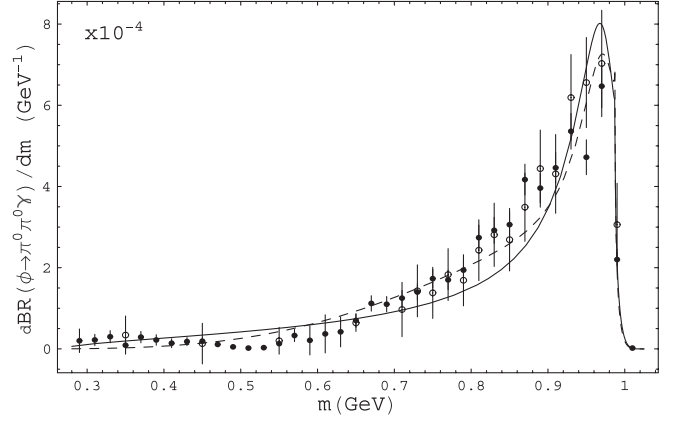


FIG. 5.  $dBR(\phi \rightarrow \pi^0 \pi^0 \gamma)/dm$  (in unit of  $\text{GeV}^{-1}$ ) as a function of the  $\pi^0$ - $\pi^0$  invariant mass  $m$  (in  $\text{GeV}^{-1}$ ). The solid line shows the best-fitted curve for the nonderivative coupling and the dashed line shows the best-fitted curve for the derivative one. Experimental data indicated by circles are from the SND collaboration in Ref. [4], and those by filled circles are from the KLEO collaboration in Ref. [4].

$$G_1 = 7.1 \times 10^{-4} \text{ GeV}^{-1},$$

$$G_2 = 0.001,$$

$$\chi^2/(\text{d.o.f}) = 131.8/(37 - 1), \quad (25)$$

$$BR(\phi \rightarrow \pi^0 \pi^0 \gamma) = 1.06 \times 10^{-4}$$

for nonderivative coupling,

$$G_1 = 6.9 \times 10^{-4} \text{ GeV}^{-1},$$

$$G_2 = 0.055,$$

$$\chi^2/(\text{d.o.f}) = 57.9/(37 - 1),$$

$$BR(\phi \rightarrow \pi^0 \pi^0 \gamma) = 1.08 \times 10^{-4}$$

for derivative coupling. (25')

The estimated value for  $BR(\phi \rightarrow \pi^0 \pi^0 \gamma)$  is consistent with the experimental data  $BR^{\text{exp}}(\phi \rightarrow \pi^0 \pi^0 \gamma) = (1.09 \pm 0.06) \times 10^{-4}$  [4,5], and the estimated value of  $G_1$  is consistent with the value evaluated from the experimental data (Ref. [5]),

$$\begin{aligned} G_1^{\text{exp}} &= \frac{2}{\pi \Gamma_f} BR^{\text{exp}}(\phi \rightarrow f_0 \gamma : m_f) BR^{\text{exp}}(f_0 \rightarrow \pi^0 \pi^0 : m_f) \\ &= (10.0 \pm 4.8) \times 10^{-4} \text{ GeV}^{-1}. \end{aligned}$$

As the case for the decay  $\phi \rightarrow \pi^0 \eta \gamma$ , pointlike  $g_{\phi f_0 \gamma}$  interaction ( $G_2$ ) is very small compared to  $|I(a, b_0)| = 0.783$  for  $m_f = 0.980$  GeV, then one can suppose that the  $K^+K^-$  loop contribution is dominant in the  $\phi \rightarrow \pi^0 \pi^0 \gamma$  decay. We suppose the  $\phi \rightarrow f_0 \gamma$  decay is caused from the  $K^+K^-$  loop interaction, then we can estimate the coupling constant  $g_{\phi K \bar{K}}$  from the relation

$$\Gamma(\phi \rightarrow f_0 \gamma) = \frac{\alpha}{3} \left| \frac{g_{\phi K \bar{K}} g_{f_0 K \bar{K}}}{2\pi^2 m_K^2} \left[ \frac{2m_K^2 - m_f^2}{2} \right] I(a, b_0) \right|^2 \times \left( \frac{m_\phi^2 - m_f^2}{2m_\phi} \right)^3, \quad (26)$$

where the factor  $\left[ \frac{2m_K^2 - m_f^2}{2} \right]$  is replaced to 1 for the non-derivative coupling. Using the value Eq. (13) of  $g_{\phi K \bar{K}}$  and the experimental value  $\Gamma(\phi \rightarrow f_0 \gamma) = (0.323 \pm 0.029) \times 10^{-3}$  MeV in Ref. [5], we obtain the result

$$g_{f_0 K \bar{K}} = \begin{cases} 4.72 \pm 0.82 \text{ GeV} & \text{for nonderivative coupling,} \\ 20.0 \pm 3.48 \text{ GeV}^{-1} & \text{for derivative coupling.} \end{cases} \quad (27)$$

Using relations Eqs. (20), (21), and (26) and estimated results (25), (25'), and (27), we obtained the values for  $g_{f_0 \pi \pi}$ ,

$$g_{f_0 \pi \pi} = \begin{cases} 1.12 \pm 0.69 \text{ GeV} & \text{for nonderivative coupling,} \\ 2.43 \pm 1.50 \text{ GeV}^{-1} & \text{for derivative coupling.} \end{cases} \quad (27')$$

The rather large value of the ratio  $g_{f_0 K \bar{K}}/g_{a_0 K \bar{K}} \sim 2$  suggests that the  $a_0$  and  $f_0$  scalar mesons are not the pure  $qq\bar{q}\bar{q}$  states but there exist the mixing (intermixing) between  $qq\bar{q}\bar{q}$  and  $q\bar{q}$  scalar mesons. Furthermore, the existence of the coupling  $g_{f_0 \pi \pi}$  suggests the intramixing between  $qq\bar{q}\bar{q}$   $f_0(600)$  and  $f_0(980)$  scalar mesons.

### III. MIXING BETWEEN LOW AND HIGH MASS SCALAR MESONS

In this section, we review the mixing among the low mass scalar, high mass scalar, and glueball discussed in our previous work [7,8]. The  $qq\bar{q}\bar{q}$  scalar  $SU(3)$  nonet  $S_a^b$  are represented by the quark triplet  $q_a$  and antiquark triplet  $\bar{q}^a$  as

$$S_b^a \sim \epsilon^{acd} q_c q_d \epsilon_{bef} \bar{q}^e \bar{q}^f \quad (28)$$

and have the following flavor configuration [6,10]:

$$\begin{aligned} \bar{d} \bar{s} s u, \frac{1}{\sqrt{2}}(\bar{d} \bar{s} d s - \bar{s} \bar{u} s u), \bar{s} \bar{u} d s &\Leftrightarrow a_0^+, a_0^0, a_0^-, \\ \bar{d} \bar{s} u d, \bar{s} \bar{u} u d, \bar{u} \bar{d} s u, \bar{u} \bar{d} d s &\Leftrightarrow \kappa^+, \kappa^0, \bar{\kappa}^0, \kappa^-, \\ \frac{1}{\sqrt{2}}(\bar{d} \bar{s} d s + \bar{s} \bar{u} s u) &\Leftrightarrow f_{NS} \sim f_0(980), \\ \bar{u} \bar{d} u d &\Leftrightarrow f_{NN} \sim f_0(600). \end{aligned}$$

The high mass scalar mesons  $S_b^a$  are the ordinary  $SU(3)$  nonet

$$S_b^a \sim \bar{q}^a q_b.$$

The intermixing between  $qq\bar{q}\bar{q}$  and  $q\bar{q}$  states may be large, because the transition between  $qq\bar{q}\bar{q}$  and  $q\bar{q}$  states is caused by the Okubo-Zweig-Iizuka (OZI) rule allowed diagram shown in Fig. 6. Considering the above flavor configuration for  $qq\bar{q}\bar{q}$  states, the expression for this tran-

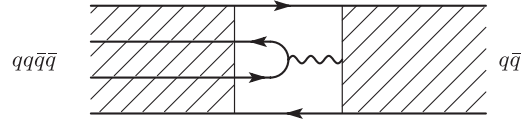


FIG. 6. OZI rule allowed graph for  $qq\bar{q}\bar{q}$  and  $q\bar{q}$  states transition.

sition is suggested as

$$\begin{aligned} L_{\text{int}} = \lambda_{01} [ &a_0^+ a_0'^- + a_0^- a_0'^+ + a_0^0 a_0'^0 + K_0^{*+} K_0'^{* -} \\ &+ K_0^{*-} K_0'^{* +} + K_0^{*0} K_0'^{* 0} + \bar{K}_0^{*0} \bar{K}_0'^{* 0} \\ &+ \sqrt{2} f_{NN} f'_N + f_{NS} f'_N + \sqrt{2} f_{NS} f'_S]. \end{aligned} \quad (29)$$

The parameter  $\lambda_{01}$  represents the strength of the intermixing and can be considered as rather large. When we represent the  $I = 1$  pure  $qq\bar{q}\bar{q}$  and  $q\bar{q}$  states by  $\overline{a_0(980)}$  and  $\overline{a_0(1450)}$ , and masses for these states by  $\frac{m^2}{a_0(980)}$  and  $\frac{m^2}{a_0(1450)}$ , the mass matrix is represented as

$$\begin{pmatrix} \frac{m^2}{a_0(980)} & \lambda_{01} \\ \lambda_{01} & \frac{m^2}{a_0(1450)} \end{pmatrix}. \quad (30)$$

Diagonalizing this mass matrix, we can get the masses for the physical states  $\overline{a_0(980)}$  and  $\overline{a_0(1450)}$  represented as mixing states of  $\overline{a_0(980)}$  and  $\overline{a_0(1450)}$ ;

$$\begin{aligned} \overline{a_0(980)} &= \cos\theta_a \overline{a_0(980)} - \sin\theta_a \overline{a_0(1450)}, \\ \overline{a_0(1450)} &= \sin\theta_a \overline{a_0(980)} + \cos\theta_a \overline{a_0(1450)}. \end{aligned} \quad (31)$$

Mixing angle  $\theta_a$  and before-mixing state masses  $\frac{m^2}{a_0(980)}$  and  $\frac{m^2}{a_0(1450)}$  are represented by the intermixing parameter  $\lambda_{01}$  as

$$\begin{aligned} \epsilon_a &= \frac{m^2_{a_0(1450)} - m^2_{a_0(980)}}{2} - \sqrt{\left( \frac{m^2_{a_0(1450)} - m^2_{a_0(980)}}{2} \right)^2 - \lambda_{01}^2}, \\ \theta_a &= \tan^{-1} \frac{\epsilon_a}{\lambda_{01}}, \quad m_{a_0(1450)} = \sqrt{m^2_{a_0(1450)} + \epsilon_a}, \\ m_{a_0(980)} &= \sqrt{m^2_{a_0(980)} - \epsilon_a}, \end{aligned} \quad (32)$$

where  $m_{a_0(980)}$  and  $m_{a_0(1450)}$  are the masses of the states  $\overline{a_0(980)}$  and  $\overline{a_0(1450)}$ .

Similarly, for the  $I = 1/2$   $K_0^*(800)$  and  $K_0^*(1430)$  mesons, the mass matrix is represented as

$$\begin{pmatrix} \frac{m^2}{K_0^*(800)} & \lambda_{01} \\ \lambda_{01} & \frac{m^2}{K_0^*(1430)} \end{pmatrix}, \quad (33)$$

where  $\frac{m^2}{K_0^*(800)}$  and  $\frac{m^2}{K_0^*(1430)}$  are the masses of pure  $qq\bar{q}\bar{q}$  and  $q\bar{q}$  states  $\overline{K_0^*(800)}$  and  $\overline{K_0^*(1430)}$ . The physical states  $\overline{K_0^*(800)}$  and  $\overline{K_0^*(1430)}$  are written by the before-mixing states  $\overline{K_0^*(800)}$  and  $\overline{K_0^*(1430)}$  and mixing angle  $\theta_K$  as

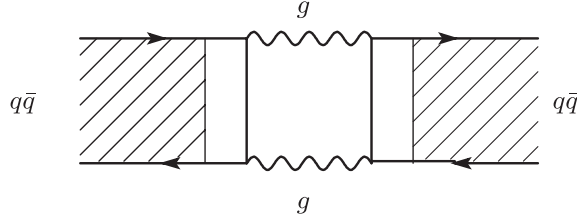


FIG. 7. OZI rule suppression graph for  $q\bar{q}$ - $q\bar{q}$  transition.

$$\begin{aligned} K_0^*(800) &= \cos\theta_K \overline{K_0^*(800)} - \sin\theta_K \overline{K_0^*(1430)}, \\ K_0^*(1430) &= \sin\theta_K \overline{K_0^*(800)} + \cos\theta_K \overline{K_0^*(1430)}. \end{aligned} \quad (34)$$

Mixing angle  $\theta_K$  and before-mixing state masses  $m_{\overline{K_0^*(800)}}$  and  $m_{\overline{K_0^*(1430)}}$  are represented by the intermixing parameter  $\lambda_{01}$  as

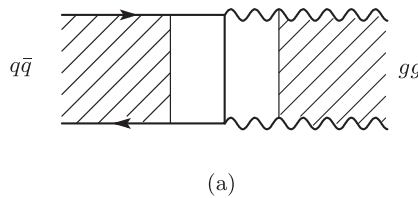
$$\begin{aligned} \epsilon_K &= \frac{m_{\overline{K_0^*(1430)}}^2 - m_{\overline{K_0^*(800)}}^2}{2} \\ &\quad - \sqrt{\left(\frac{m_{\overline{K_0^*(1430)}}^2 - m_{\overline{K_0^*(800)}}^2}{2}\right)^2 - \lambda_{01}^2}, \end{aligned} \quad (35)$$

$$\begin{aligned} \theta_K &= \tan^{-1} \frac{\epsilon_K}{\lambda_{01}}, \quad m_{\overline{K_0^*(1430)}} = \sqrt{m_{\overline{K_0^*(1430)}}^2 + \epsilon_K}, \\ m_{\overline{K_0^*(800)}} &= \sqrt{m_{\overline{K_0^*(800)}}^2 - \epsilon_K}, \end{aligned}$$

where  $m_{\overline{K_0^*(800)}}$  and  $m_{\overline{K_0^*(1430)}}$  are the masses of the physical states  $K_0^*(800)$  and  $K_0^*(1430)$ .

Next, we consider the mixing between  $I = 0$  low and high mass scalar mesons. Among the  $I = 0$ ,  $L = 1q\bar{q}$  scalar mesons, there are the intramixing weaker than the intermixing, caused from the transition between themselves represented by the OZI rule suppression graph shown in Fig. 7, and furthermore the mixing between the  $q\bar{q}$  scalar meson and the glueball caused from the transition represented by the graph shown in Fig. 8(a). Thus, the mass matrix for these  $I = 0$ ,  $L = 1q\bar{q}$  scalar mesons and the glueball is represented as

$$\begin{pmatrix} m_{N'}^2 + 2\lambda_1 & \sqrt{2}\lambda_1 & \sqrt{2}\lambda_G \\ \sqrt{2}\lambda_1 & m_{S'}^2 + \lambda_1 & \lambda_G \\ \sqrt{2}\lambda_G & \lambda_G & \lambda_{GG} \end{pmatrix}, \quad \begin{aligned} m_{N'}^2 &= m_{a_0(1450)}^2, \\ m_{S'}^2 &= 2m_{\overline{K_0^*(1430)}}^2 - m_{a_0(1450)}^2, \end{aligned} \quad (36)$$



(a)

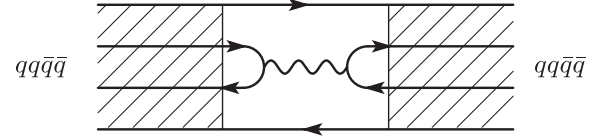


FIG. 9. OZI suppression graph for  $qq\bar{q}\bar{q}$ - $qq\bar{q}\bar{q}$  transition.

where  $\lambda_1$  is the transition strength among the  $I = 0$   $q\bar{q}$  mesons,  $\lambda_G$  is the transition strength between  $q\bar{q}$  and the glueball  $gg$ , and  $\lambda_{GG}$  is the pure glueball mass square. For the light  $I = 0$   $qq\bar{q}\bar{q}$  scalar mesons, there are the intramixing caused from the transition between themselves represented by the OZI rule suppression graph shown in Fig. 9, and the mass matrix for these  $I = 0$   $qq\bar{q}\bar{q}$  scalar mesons is represented as

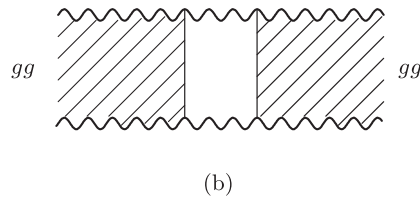
$$\begin{pmatrix} m_{NN}^2 + \lambda_0 & \sqrt{2}\lambda_0 \\ \sqrt{2}\lambda_0 & m_{NS}^2 + 2\lambda_0 \end{pmatrix}, \quad \begin{aligned} m_{NN}^2 &= 2m_{\overline{K_0^*(800)}}^2 - m_{a_0(980)}^2, \\ m_{NS}^2 &= m_{a_0(980)}^2, \end{aligned} \quad (37)$$

where  $\lambda_0$  represents the transition strength between  $I = 0$   $qq\bar{q}\bar{q}$  mesons.

The intermixing and intramixing among  $I = 0$  low mass and high mass scalar mesons and the glueball is expressed by the overall mixing mass matrix as

$$\begin{pmatrix} m_{NN}^2 + \lambda_0 & \sqrt{2}\lambda_0 & \sqrt{2}\lambda_{01} & 0 & 0 \\ \sqrt{2}\lambda_0 & m_{NS}^2 + 2\lambda_0 & \lambda_{01} & \sqrt{2}\lambda_{01} & 0 \\ \sqrt{2}\lambda_{01} & \lambda_{01} & m_{N'}^2 + 2\lambda_1 & \sqrt{2}\lambda_1 & \sqrt{2}\lambda_G \\ 0 & \sqrt{2}\lambda_{01} & \sqrt{2}\lambda_1 & m_{S'}^2 + \lambda_1 & \lambda_G \\ 0 & 0 & \sqrt{2}\lambda_G & \lambda_G & \lambda_{GG} \end{pmatrix}. \quad (38)$$

Diagonalizing this mass matrix, we obtain the eigenvalues of low mass and high mass scalar mesons  $I = 0$  states  $f_0(600)$ ,  $f_0(980)$ ,  $f_0(1370)$ ,  $f_0(1500)$ , and  $f_0(1710)$ . The eigenstates of these scalar mesons are represented as follows:



(b)

FIG. 8. Transition graph between (a)  $q\bar{q}$  and  $gg$ , and (b)  $gg$  and  $gg$ .

$$\begin{pmatrix} f_0(600) \\ f_0(980) \\ f_0(1370) \\ f_0(1500) \\ f_0(1710) \end{pmatrix} = [R_{f_0(M)I}] \begin{pmatrix} f_{NN} \\ f_{NS} \\ f_{N'} \\ f_{S'} \\ f_G \end{pmatrix}, \quad [R_{f_0(M)I}] = \begin{pmatrix} R_{f_0(600)NN} & R_{f_0(600)NS} & R_{f_0(600)N'} & R_{f_0(600)S'} & R_{f_0(600)G} \\ R_{f_0(980)NN} & R_{f_0(980)NS} & R_{f_0(980)N'} & R_{f_0(980)S'} & R_{f_0(980)G} \\ R_{f_0(1370)NN} & R_{f_0(1370)NS} & R_{f_0(1370)N'} & R_{f_0(1370)S'} & R_{f_0(1370)G} \\ R_{f_0(1500)NN} & R_{f_0(1500)NS} & R_{f_0(1500)N'} & R_{f_0(1500)S'} & R_{f_0(1500)G} \\ R_{f_0(1710)NN} & R_{f_0(1710)NS} & R_{f_0(1710)N'} & R_{f_0(1710)S'} & R_{f_0(1710)G} \end{pmatrix}. \quad (39)$$

Using the intermixing parameter  $\lambda_{01}$  and the mass values,  $m_{a_0(980)} = (0.9848 \pm 0.0012)$  GeV,  $m_{a_0(1450)} = (1.474 \pm 0.019)$  GeV,  $m_{K_0^*(800)} = (0.841 \pm 0.030)$  GeV, and  $m_{K_0^*(1430)} = (1.414 \pm 0.006)$  GeV, we obtained the mixing angles  $\theta_a$ ,  $\theta_K$  and before-mixing states masses  $m_{\overline{a_0(980)}}$ ,  $m_{\overline{a_0(1450)}}$ ,  $m_{\overline{K_0^*(800)}}$ ,  $m_{\overline{K_0^*(1430)}}$  from the relations (32) and (35). Using the values of  $m_{N'}^2$ ,  $m_{S'}^2$ ,  $m_{NN}^2$ , and  $m_{NS}^2$  obtained from the second equations in Eqs. (36) and (37), and parameters  $\lambda_0$ ,  $\lambda_1$ ,  $\lambda_G$ , and  $\lambda_{GG}$ , we diagonalize the mass matrix Eq. (38). When we fit the eigenvalues obtained to the following experimental mass values [5],

$$\begin{aligned} m_{f_0(600)} &= 0.80 \pm 0.40 \text{ GeV}, \\ m_{f_0(980)} &= 0.980 \pm 0.010 \text{ GeV}, \\ m_{f_0(1370)} &= 1.350 \pm 0.150 \text{ GeV}, \\ m_{f_0(1500)} &= 1.507 \pm 0.005 \text{ GeV}, \\ m_{f_0(1710)} &= 1.718 \pm 0.006 \text{ GeV}, \end{aligned} \quad (40)$$

we obtain the allowed values for  $\lambda_0$ ,  $\lambda_1$ ,  $\lambda_G$ , and  $\lambda_{GG}$ . We tabulated the  $\theta_a$ ,  $\theta_K$ ,  $\lambda_0$ ,  $\lambda_1$ ,  $\lambda_G$ ,  $\lambda_{GG}$  and  $R_{f_0(980)NN}$ ,  $R_{f_0(980)NS}$ ,  $R_{f_0(980)N'}$ ,  $R_{f_0(980)S'}$ ,  $R_{f_0(980)G}$  for the various values of  $\lambda_{01}$  in the Table I.

TABLE I. The values of mixing angles  $\theta_a$ ,  $\theta_K$ , and the transition parameters  $\lambda_0$ ,  $\lambda_1$ ,  $\lambda_G$ ,  $\lambda_{GG}$ , and mixing parameters  $R_{f_0(980)NN}$ ,  $R_{f_0(980)NS}$ ,  $R_{f_0(980)N'}$ ,  $R_{f_0(980)S'}$ ,  $R_{f_0(980)G}$  for the various values of  $\lambda_{01}$ .

$\lambda_{01}$ (GeV <sup>2</sup> )	$\theta_a$ (°)	$\theta_K$ (°)	$\lambda_0$ (GeV <sup>2</sup> )	$\lambda_1$ (GeV <sup>2</sup> )	$\lambda_G$ (GeV <sup>2</sup> )	$\lambda_{GG}$ (GeV <sup>2</sup> )
	$R_{f_0(980)NN}$	$R_{f_0(980)NS}$	$R_{f_0(980)N'}$	$R_{f_0(980)S'}$	$R_{f_0(980)G}$	
0.20	$9.7 \pm 0.5$	$9.0 \pm 0.5$	$0.018 \pm 0.009$	$0.275 \pm 0.007$	$0.04 \pm 0.04$	$(1.152 \pm 0.008)^2$
	$-0.023 \pm 0.014$	$-0.972 \pm 0.002$	$0.065 \pm 0.006$	$0.226 \pm 0.004$	$-0.010 \pm 0.010$	
0.25	$12.3 \pm 0.6$	$11.4 \pm 0.6$	$0.032 \pm 0.010$	$0.264 \pm 0.008$	$0.05 \pm 0.05$	$(1.512 \pm 0.007)^2$
	$-0.027 \pm 0.026$	$-0.954 \pm 0.003$	$0.086 \pm 0.008$	$0.284 \pm 0.005$	$-0.016 \pm 0.016$	
0.30	$15.0 \pm 0.8$	$13.8 \pm 0.8$	$0.050 \pm 0.009$	$0.252 \pm 0.009$	$0.04 \pm 0.04$	$(1.512 \pm 0.008)^2$
	$-0.046 \pm 0.024$	$-0.932 \pm 0.004$	$0.110 \pm 0.009$	$0.341 \pm 0.006$	$-0.016 \pm 0.016$	
0.35	$17.8 \pm 1.0$	$16.4 \pm 1.0$	$0.072 \pm 0.012$	$0.233 \pm 0.008$	$0.05 \pm 0.05$	$(1.511 \pm 0.008)^2$
	$-0.065 \pm 0.025$	$-0.902 \pm 0.007$	$0.140 \pm 0.012$	$0.401 \pm 0.007$	$-0.024 \pm 0.024$	
0.40	$20.8 \pm 1.2$	$19.1 \pm 1.2$	$0.104 \pm 0.012$	$0.213 \pm 0.009$	$0.05 \pm 0.05$	$(1.509 \pm 0.006)^2$
	$-0.094 \pm 0.021$	$-0.864 \pm 0.010$	$0.178 \pm 0.014$	$0.461 \pm 0.007$	$-0.028 \pm 0.028$	
0.45	$24.2 \pm 1.6$	$22.1 \pm 1.5$	$0.146 \pm 0.014$	$0.178 \pm 0.007$	$0.04 \pm 0.04$	$(1.506 \pm 0.002)^2$
	$-0.116 \pm 0.021$	$-0.813 \pm 0.011$	$0.226 \pm 0.015$	$0.523 \pm 0.006$	$-0.014 \pm 0.014$	

#### IV. COUPLING CONSTANT $g_{SPP}$ AND MIXING BETWEEN $qq\bar{q}\bar{q}$ AND $q\bar{q}$ SCALAR MESONS

In this section, we first express the  $g_{SPP}$ 's by the mixing angle  $\theta_a$ ,  $\theta_K$  and mixing parameters  $R_{f_0NS}$ , etc. Next, we obtain the values of the  $g_{SPP}$  using the various  $S \rightarrow PP$  decay widths and compare these values with the ones obtained from  $\phi$  decay, and then suggest the importance of the mixing between  $qq\bar{q}\bar{q}$  and  $q\bar{q}$  scalar mesons.

We use the following expressions for  $S(qq\bar{q}\bar{q}$  scalar meson) $PP$ ,  $S'(q\bar{q}$  scalar meson) $PP$ , and  $G$ (pure glueball) $PP$  coupling with coupling constants  $A$ ,  $A'$ , and  $A''$ , respectively [6,8],

$$L_I = A\varepsilon^{abc}\varepsilon_{def}S_a^dP_b^eP_c^f + A'S_a^{lb}\{P_b^c, P_c^a\} + A''G\{P_a^b, P_b^a\} \quad \text{for nonderivative coupling}, \quad (41)$$

$$A\varepsilon^{abc}\varepsilon_{def}S_a^d\partial^\mu P_b^e\partial_\mu P_c^f + A'S_a^{lb}\{\partial^\mu P_b^c, \partial_\mu P_c^a\} + A''G\{\partial^\mu P_a^b, \partial_\mu P_b^a\} \quad \text{for derivative coupling}. \quad (41')$$

These interactions are represented graphically by the diagrams shown in Fig. 10. We define the coupling constants  $g_{SPP'}$  in the following expression:

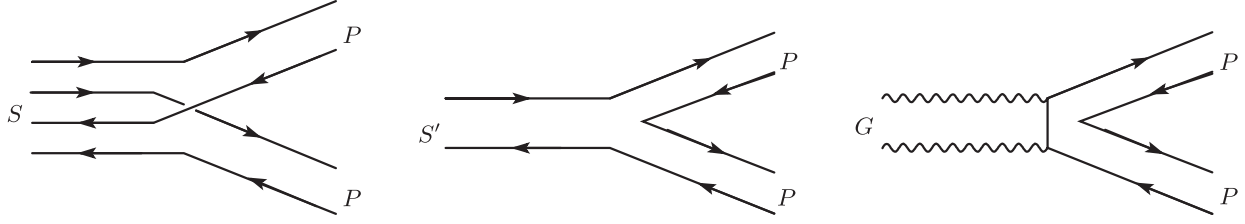


FIG. 10. *SPP*, *S'PP*, and *GPP* coupling.

$$\begin{aligned}
 L_I = & g_{a_0 K \bar{K}} [\partial^\mu] \bar{K} \boldsymbol{\tau} \cdot \mathbf{a}_0 [\partial_\mu] K + g_{a'_0 K \bar{K}} [\partial^\mu] \bar{K} \boldsymbol{\tau} \cdot \mathbf{a}'_0 [\partial_\mu] K + g_{a_0 \pi \eta} \mathbf{a}_0 \cdot [\partial^\mu] \boldsymbol{\pi} [\partial_\mu] \eta + g_{a'_0 \pi \eta} \mathbf{a}'_0 \cdot [\partial^\mu] \boldsymbol{\pi} [\partial_\mu] \eta \\
 & + g_{a_0 \pi \eta'} \mathbf{a}_0 \cdot [\partial^\mu] \boldsymbol{\pi} [\partial_\mu] \eta' + g_{a'_0 \pi \eta'} \mathbf{a}'_0 \cdot [\partial^\mu] \boldsymbol{\pi} [\partial_\mu] \eta' + g_{K_0^* K \pi} ([\partial^\mu] \bar{K} \boldsymbol{\tau} \cdot [\partial_\mu] \boldsymbol{\pi} K_0^* + \text{H.c.}) \\
 & + g_{K_0^* K \pi} ([\partial^\mu] \bar{K} \boldsymbol{\tau} \cdot [\partial_\mu] \boldsymbol{\pi} K_0^{*'} + \text{H.c.}) + g_{K_0^* K \eta} (\bar{K}_0^* [\partial^\mu] K [\partial_\mu] \eta + \text{H.c.}) + g_{K_0^* K \eta} (\bar{K}_0^{*'} [\partial^\mu] K [\partial_\mu] \eta + \text{H.c.}) \\
 & + g_{K_0^* K \eta'} (\bar{K}_0^* [\partial^\mu] K [\partial_\mu] \eta' + \text{H.c.}) + g_{K_0^* K \eta'} (\bar{K}_0^{*'} [\partial^\mu] K [\partial_\mu] \eta' + \text{H.c.}) + g_{f_0(M) \pi \pi} \frac{1}{2} f_0(M) [\partial^\mu] \boldsymbol{\pi} \cdot [\partial_\mu] \boldsymbol{\pi} \\
 & + g_{f_0(M) K \bar{K}} f_0(M) [\partial^\mu] K [\partial_\mu] \bar{K} + g_{f_0(M) \eta \eta} f_0(M) [\partial^\mu] \eta [\partial_\mu] \eta + g_{f_0(M) \eta \eta'} f_0(M) [\partial^\mu] \eta [\partial_\mu] \eta' \\
 & + g_{f_0(M) \eta' \eta'} f_0(M) [\partial^\mu] \eta' [\partial_\mu] \eta',
 \end{aligned} \tag{42}$$

where  $[\partial^\mu]$ 's are replaced to 1 for nonderivative couplings. These definitions of  $g_{SPP}$ 's are the same as the ones of  $\gamma_{SPP}$  in our previous work [8] except for  $g_{a_0 K \bar{K}}$ ,  $g_{K_0^* K \pi}$ , which are related as  $\sqrt{2} g_{a_0 K \bar{K}} = \gamma_{a_0 K \bar{K}}$ ,  $\sqrt{2} g_{K_0^* K \pi} = \gamma_{K_0^* K \pi}$ .

Then the coupling constants  $g_{SPP}$ 's are expressed as

$$\begin{aligned}
 g_{a_0(980) K \bar{K}} &= \sqrt{2}(A \cos \theta_a - A' \sin \theta_a), & g_{a_0(1450) K \bar{K}} &= \sqrt{2}(A \sin \theta_a + A' \cos \theta_a), \\
 g_{a_0(980) \pi \eta} &= 2(A \cos \theta_a \sin \theta_P - \sqrt{2} A' \sin \theta_a \cos \theta_P), & g_{a_0(1450) \pi \eta} &= 2(A \sin \theta_a \sin \theta_P + \sqrt{2} A' \cos \theta_a \cos \theta_P), \\
 g_{a_0(1450) \pi \eta'} &= 2(-A \sin \theta_a \cos \theta_P + \sqrt{2} A' \cos \theta_a \sin \theta_P), & g_{K_0^*(800) \pi K} &= \sqrt{2}(A \cos \theta_K - A' \sin \theta_K), \\
 g_{K_0^*(1430) \pi K} &= \sqrt{2}(A \sin \theta_K + A' \cos \theta_K), & g_{f_0(M) \pi \pi} &= 2(-AR_{f_0(M) NN} + \sqrt{2} A' R_{f_0(M) N'} + 2A'' R_{f_0(M) G}), \\
 g_{f_0(M) K \bar{K}} &= \sqrt{2}(-AR_{f_0(M) NS} + A' R_{f_0(M) N'} + \sqrt{2} A' R_{f_0(M) S'} + 2\sqrt{2} A'' R_{f_0(M) G}), \\
 g_{f_0(M) \eta \eta} &= 2(-AR_{f_0(M) NS} \cos \theta_P \sin \theta_P + \frac{1}{2} AR_{f_0(M) NN} \cos^2 \theta_P + \frac{1}{\sqrt{2}} A' R_{f_0(M) N'} \cos^2 \theta_P + A' R_{f_0(M) S'} \sin^2 \theta_P + A'' R_{f_0(M) G}), \\
 g_{f_0(M) \eta \eta'} &= 2(AR_{f_0(M) NS} \cos 2\theta_P + \frac{1}{2} AR_{f_0(M) NN} \sin 2\theta_P + \frac{1}{\sqrt{2}} A' R_{f_0(M) N'} \sin 2\theta_P - A' R_{f_0(M) S'} \sin 2\theta_P), \\
 g_{f_0(M) \eta' \eta'} &= 2\left(AR_{f_0(M) NS} \cos \theta_P \sin \theta_P + \frac{1}{2} AR_{f_0(M) NN} \sin^2 \theta_P + \frac{1}{\sqrt{2}} A' R_{f_0(M) N'} \sin^2 \theta_P + A' R_{f_0(M) S'} \cos^2 \theta_P + A'' R_{f_0(M) G}\right),
 \end{aligned} \tag{43}$$

where  $\theta_P$  is the  $\eta$ - $\eta'$  mixing angle related to the traditional octet-singlet mixing angle  $\theta_{0-8}$  as  $\theta_P = \theta_{0-8} + 54.7^\circ$ .

Decay widths for these scalar mesons are expressed by using the coupling constant  $g_{SPP}$  as

TABLE II. The results of the best-fit analyses for the nonderivative coupling case. The experimental data of the scalar meson decay widths used are cited in Ref. [5]. For the  $\theta_p$ , we search the best-fit value in the range  $(54.7 \pm 18)^\circ$ . The values of  $g_{a_0(980)\pi\eta}$ , etc. are the ones obtained for  $\phi \rightarrow a_0(980)\gamma/\pi^0\eta\gamma$  and  $\phi \rightarrow f_0(980)\gamma/\pi^0\pi^0\gamma$  decay analysis.

$\lambda_{01}$ (GeV <sup>2</sup> )	$A$ GeV	$A'$ GeV	$A''$ GeV	$\theta_p$ degree (°)	$\Gamma_{a_0(980)\rightarrow\pi\eta+K\bar{K}}$ $0.075 \pm 0.025$ GeV
0.20	2.8	1.2	-0.25	36.7	0.189
0.25	2.5	1.2	-0.23	36.7	0.133
0.30	2.3	1.2	-0.24	36.7	0.097
0.35	1.9	1.3	-0.24	50.2	0.081
0.40	1.7	1.3	-0.24	59.2	0.072
0.45	1.5	1.4	-0.26	72.7	0.068
	$\Gamma_{a_0(1450)\rightarrow\pi\eta+\pi\eta'+K\bar{K}}$	$\Gamma_{K_0^*(1430)\rightarrow\pi K}$	$\Gamma_{f_0(980)\rightarrow\pi\pi+K\bar{K}}$	$\Gamma_{f_0(1370)\rightarrow\pi\pi+K\bar{K}+\eta\eta}$	$\Gamma_{f_0(1500)\rightarrow\pi\pi+K\bar{K}+\eta\eta+\eta\eta'}$
	$0.265 \pm 0.013$ GeV	$0.270 \pm 0.043$ GeV	$0.070 \pm 0.030$ GeV	$0.214 \pm 0.120$ GeV	$0.055 \pm 0.009$ GeV
0.20	0.242	0.192	0.119	0.034	0.063
0.25	0.250	0.204	0.107	0.031	0.057
0.30	0.258	0.214	0.104	0.029	0.055
0.35	0.273	0.232	0.098	0.034	0.058
0.40	0.263	0.233	0.098	0.040	0.054
0.45	0.272	0.253	0.124	0.084	0.056
	$\Gamma_{f_0(1710)\rightarrow\pi\pi+K\bar{K}+\eta\eta}$	$g_{a_0(980)K\bar{K}}$	$g_{a_0(980)\pi\eta}$	$g_{f_0(980)K\bar{K}}$	$g_{f_0(980)\pi\pi}$
	$0.137 \pm 0.008$ GeV	$2.18 \pm 0.12$ GeV	$1.89 \pm 0.75$ GeV	$4.72 \pm 0.82$ GeV	$1.12 \pm 0.69$ GeV
0.20	0.177	3.62	2.84	4.51	0.31
0.25	0.156	3.09	2.34	4.21	0.45
0.30	0.140	2.70	1.95	4.05	0.61
0.35	0.151	2.00	2.06	3.74	0.78
0.40	0.129	1.59	2.06	3.63	1.00
0.45	0.141	1.12	2.13	3.66	1.27

TABLE III. The results of the best-fit analyses for the derivative coupling case. The experimental data of the scalar meson decay widths used are cited in Ref. [5]. For the  $\theta_p$ , we search the best-fit value in the range  $(54.7 \pm 18)^\circ$ . The values of  $g_{a_0(980)\pi\eta}$ , etc. are the ones obtained for  $\phi \rightarrow a_0(980)\gamma/\pi^0\eta\gamma$  and  $\phi \rightarrow f_0(980)\gamma/\pi^0\pi^0\gamma$  decay analysis.

$\lambda_{01}$ (GeV <sup>2</sup> )	$A$ GeV <sup>-1</sup>	$A'$ GeV <sup>-1</sup>	$A''$ GeV <sup>-1</sup>	$\theta_p$ degree (°)	$\Gamma_{a_0(980)\rightarrow\pi\eta+K\bar{K}}$ $0.075 \pm 0.025$ GeV
0.20	5.8	1.2	-0.26	41.2	0.093
0.25	8.3	0.57	-0.37	36.7	0.170
0.30	7.2	0.51	-0.33	36.7	0.124
0.35	6.0	0.54	-0.35	36.7	0.068
0.40	5.1	0.57	-0.36	36.7	0.054
0.45	4.2	0.59	-0.34	50.2	0.051
	$\Gamma_{a_0(1450)\rightarrow\pi\eta+\pi\eta'+K\bar{K}}$	$\Gamma_{K_0^*(1430)\rightarrow\pi K}$	$\Gamma_{f_0(980)\rightarrow\pi\pi+K\bar{K}}$	$\Gamma_{f_0(1370)\rightarrow\pi\pi+K\bar{K}+\eta\eta}$	$\Gamma_{f_0(1500)\rightarrow\pi\pi+K\bar{K}+\eta\eta+\eta\eta'}$
	$0.265 \pm 0.013$ GeV	$0.270 \pm 0.043$ GeV	$0.070 \pm 0.030$ GeV	$0.214 \pm 0.120$ GeV	$0.055 \pm 0.009$ GeV
0.20	0.276	0.239	0.025	0.009	0.057
0.25	0.274	0.262	0.045	0.083	0.068
0.30	0.279	0.267	0.036	0.099	0.053
0.35	0.279	0.266	0.028	0.090	0.055
0.40	0.279	0.266	0.025	0.082	0.059
0.45	0.276	0.246	0.022	0.056	0.057
	$\Gamma_{f_0(1710)\rightarrow\pi\pi+K\bar{K}+\eta\eta}$	$g_{a_0(980)K\bar{K}}$	$g_{a_0(980)\pi\eta}$	$g_{f_0(980)K\bar{K}}$	$g_{f_0(980)\pi\pi}$
	$0.137 \pm 0.008$ GeV	$9.04 \pm 0.50$ GeV <sup>-1</sup>	$5.79 \pm 2.32$ GeV <sup>-1</sup>	$20.0 \pm 3.48$ GeV <sup>-1</sup>	$2.43 \pm 1.50$ GeV <sup>-1</sup>
0.20	0.158	7.80	7.10	8.63	0.39
0.25	0.106	11.3	9.42	11.6	0.65
0.30	0.152	9.65	8.02	9.94	0.87
0.35	0.152	7.85	6.45	8.23	1.03
0.40	0.152	6.45	5.24	6.94	1.28
0.45	0.132	5.07	5.45	5.67	1.39

$$\begin{aligned}
 \Gamma(a_0(M) \rightarrow K^+(m_1)K^-(m_2) + K^0(m_1)\bar{K}^0(m_2)) &= 2 \frac{g_{a_0(M)K\bar{K}}^2}{8\pi} \frac{|\mathbf{q}|}{m_{a_0(M)}^2} \left[ \left( \frac{m_{Mm_1m_2}^2}{2} \right)^2 \right], \\
 \Gamma(a_0(M) \rightarrow \pi(m_1) + \eta(m_2)) &= \frac{g_{a_0(M)\pi\eta}^2}{8\pi} \frac{|\mathbf{q}|}{m_{a_0(M)}^2} \left[ \left( \frac{m_{Mm_1m_2}^2}{2} \right)^2 \right], \\
 \Gamma(a_0(M) \rightarrow \pi(m_1) + \eta'(m_2)) &= \frac{g_{a_0(M)\pi\eta'}^2}{8\pi} \frac{|\mathbf{q}|}{m_{a_0(M)}^2} \left[ \left( \frac{m_{Mm_1m_2}^2}{2} \right)^2 \right], \\
 \Gamma(K_0^{*+}(M) \rightarrow \pi^+(m_1)K^0(m_2) + \pi^0(m_1)K^+(m_2)) &= 3 \frac{g_{K_0^{*+}(M)\pi K}^2}{8\pi} \frac{|\mathbf{q}|}{m_{K_0^{*+}(M)}^2} \left[ \left( \frac{m_{Mm_1m_2}^2}{2} \right)^2 \right], \\
 \Gamma(f_0(M) \rightarrow \pi^+(m_1)\pi^-(m_2) + \pi^0(m_1)\pi^0(m_2)) &= \frac{3}{2} \frac{g_{f_0(M)\pi\pi}^2}{8\pi} \frac{|\mathbf{q}|}{m_{f_0(M)}^2} \left[ \left( \frac{m_{Mm_1m_2}^2}{2} \right)^2 \right], \\
 \Gamma(f_0(M) \rightarrow K^+(m_1)K^-(m_2) + K^0(m_1)\bar{K}^0(m_2)) &= 2 \frac{g_{f_0(M)K\bar{K}}^2}{8\pi} \frac{|\mathbf{q}|}{m_{f_0(M)}^2} \left[ \left( \frac{m_{Mm_1m_2}^2}{2} \right)^2 \right], \\
 \Gamma(f_0(M) \rightarrow \eta(m_1) + \eta(m_2)) &= 2 \frac{g_{f_0(M)\eta\eta}^2}{8\pi} \frac{|\mathbf{q}|}{m_{f_0(M)}^2} \left[ \left( \frac{m_{Mm_1m_2}^2}{2} \right)^2 \right], \\
 \Gamma(f_0(M) \rightarrow \eta(m_1) + \eta'(m_2)) &= \frac{g_{f_0(M)\eta\eta'}^2}{8\pi} \frac{|\mathbf{q}|}{m_{f_0(M)}^2} \left[ \left( \frac{m_{Mm_1m_2}^2}{2} \right)^2 \right], \\
 \Gamma(f_0(M) \rightarrow \eta'(m_1) + \eta'(m_2)) &= 2 \frac{g_{f_0(M)\eta'\eta'}^2}{8\pi} \frac{|\mathbf{q}|}{m_{f_0(M)}^2} \left[ \left( \frac{m_{Mm_1m_2}^2}{2} \right)^2 \right].
 \end{aligned} \tag{44}$$

Here  $|\mathbf{q}|$  and  $m_{Mm_1m_2}$  are defined as

$$\begin{aligned}
 |\mathbf{q}| &= \sqrt{\left( \frac{M^2 + m_2^2 - m_1^2}{2M} \right)^2 - m_2^2}, \\
 m_{Mm_1m_2} &= \sqrt{M^2 - m_1^2 - m_2^2},
 \end{aligned}$$

and for the case  $M \approx m_1 + m_2$ , we use the next formula for  $|\mathbf{q}|$  [11],

$$\begin{aligned}
 |\mathbf{q}| &= \text{Re} \frac{1}{\sqrt{2\pi}\Gamma_M} \int_{M-\infty}^{M+\infty} e^{-[(m-M)^2/2\Gamma_M^2]} \\
 &\times \sqrt{\left( \frac{M^2 + m_2^2 - m_1^2}{2M} \right)^2 - m_2^2} dm, \tag{45}
 \end{aligned}$$

where  $\Gamma_M$  is the decay width of the particle with mass  $M$ .

We use the experimental data of the scalar meson decays cited in Ref. [5];  $\Gamma(a_0(980) \rightarrow \pi\eta + K\bar{K}) = 75 \pm 25$  MeV,  $\Gamma(a_0(1450) \rightarrow \pi\eta + \pi\eta' + K\bar{K}) = 265 \pm 13$  MeV,  $\Gamma(K_0^*(1430) \rightarrow \pi K) = 270 \pm 43$  MeV [12],  $\Gamma(f_0(980) \rightarrow \pi\pi + K\bar{K}) = 70 \pm 30$  MeV,  $\Gamma(f_0(1370) \rightarrow \pi\pi + K\bar{K} + \eta\eta) = 214 \pm 120$  MeV [13],  $\Gamma(f_0(1500) \rightarrow \pi\pi + K\bar{K} + \eta\eta + \eta\eta') = 55 \pm 9$  MeV [14],  $\Gamma(f_0(1710) \rightarrow \pi\pi + K\bar{K} + \eta\eta) = 137 \pm 8$  MeV, for the best fitting of our model parameters,  $A$ ,  $A'$ ,  $A''$ , and  $\theta_p$ . Results are tabulated in Table II for the nonderivative coupling case and in Table III for the derivative coupling case. For the  $\theta_p$ , we search the best-fit value in the range  $(54.7 \pm 18)^\circ$ . We estimate the best-fit values of these parameters for various

points (0.2, 0.25, 0.30, 0.35, 0.40, 0.45)  $\text{GeV}^2$  of the intermixing parameter  $\lambda_{01}$ . We show the values of  $\Gamma(a_0(980) \rightarrow \pi\eta + K\bar{K})$ , etc. and  $g_{a_0(980)\pi\eta}$ , etc. for best-fitted  $A$ ,  $A'$ ,  $A''$ , and  $\theta_p$ . Values in the row just below the one denoting  $\Gamma(a_0(980) \rightarrow \pi\eta + K\bar{K})$ , etc. denote the experimental values and the values in the row just below the one denoting  $g_{a_0(980)\pi\eta}$ , etc. are the values Eqs. (18), (18'), (27), and (27') obtained from  $\phi \rightarrow a_0\gamma/\pi^0\eta\gamma$  and  $\phi \rightarrow f_0\gamma/\pi^0\pi^0\gamma$  decay analyses.

These results in Table II (nonderivative coupling case) show that the values of  $g_{a_0(980)\pi\eta}$ , etc. obtained for  $\lambda_{01} = 0.30 \sim 0.35$  ( $\text{GeV}^2$ ) are close to the values obtained in  $\phi \rightarrow a_0\gamma/\pi^0\eta\gamma$  and  $\phi \rightarrow f_0\gamma/\pi^0\pi^0\gamma$  decay analyses. For the derivative coupling case (showed in Table III), the values of  $g_{a_0(980)\pi\eta}$ , etc. except for  $g_{f_0(980)K\bar{K}}$  obtained for  $\lambda_{01} = 0.30 \sim 0.35$  ( $\text{GeV}^2$ ) are also close to the values obtained in the  $\phi \rightarrow a_0\gamma/\pi^0\eta\gamma$  and  $\phi \rightarrow f_0\gamma/\pi^0\pi^0\gamma$  decay analyses. But the characteristic feature  $g_{f_0(980)K\bar{K}}/g_{a_0(980)K\bar{K}} \sim 2$  obtained in  $\phi \rightarrow a_0\gamma/\pi^0\eta\gamma$  and  $\phi \rightarrow f_0\gamma/\pi^0\pi^0\gamma$  decay analyses cannot be taken in any values of  $\lambda_{01}$  for the derivative coupling case.

## V. CONCLUSION

From the invariant mass distribution analysis of radiative decays  $\phi \rightarrow a_0(980)\gamma \rightarrow \pi^0\eta\gamma$  and  $\phi \rightarrow f_0(980)\gamma \rightarrow \pi^0\pi^0\gamma$ , we obtain the results that the  $K\bar{K}$  loop diagram contribution for  $\phi a_0\gamma$  and  $\phi f_0\gamma$  couplings are dominant for both nonderivative and derivative  $SPP$  coupling cases.

We assume that  $\phi \rightarrow a_0(980)\gamma$  and  $\phi \rightarrow f_0(980)\gamma$  decays are caused through only the  $K\bar{K}$  loop diagram, and then we get the results Eqs. (18), (18'), (27), and (27') of *SPP* coupling constants,

	Nonderivative coupling	Derivative coupling
$g_{a_0 K\bar{K}}$	$2.18 \pm 0.12 \text{ GeV}$	$9.04 \pm 0.50 \text{ GeV}^{-1}$
$g_{a_0 \pi\eta}$	$1.89 \pm 0.75 \text{ GeV}$	$5.79 \pm 2.32 \text{ GeV}^{-1}$
$g_{f_0 K\bar{K}}$	$4.72 \pm 0.82 \text{ GeV}$	$20.0 \pm 3.48 \text{ GeV}^{-1}$
$g_{f_0 \pi\pi}$	$1.12 \pm 0.69 \text{ GeV}$	$2.43 \pm 1.50 \text{ GeV}^{-1}$

We consider that the scalar  $a_0(980)$  and  $f_0(980)$  are  $q\bar{q}\bar{q}$  states and mix with high mass scalar mesons con-

sidered as  $q\bar{q}$  states. The low mass scalar and high mass scalar mesons are considered to mix through the intermixing parameter  $\lambda_{01}$ . In our mass formula, we obtain the mixing angle  $\theta_a$ ,  $\theta_K$  and mixing parameters  $R_{f_0(980)NN}$ 's using the mass values of low mass scalar mesons ( $a_0(980)$ ,  $K_0^*(800)$ ,  $f_0(600)$ ,  $f_0(980)$ ) and high mass scalar mesons and glueball ( $a_0(1450)$ ,  $K_0^*(1430)$ ,  $f_0(1370)$ ,  $f_0(1500)$ ,  $f_0(1710)$ ). We tabulate these values for  $\lambda_{01} = (0.30 \leftrightarrow 0.35) \text{ GeV}^2$ .

$$\theta_a = (15.0 \leftrightarrow 17.8)^\circ, \quad \theta_K = (13.8 \leftrightarrow 16.4)^\circ,$$

	$f_{NN}$	$f_{NS}$	$f_{N'}$	$f_{S'}$	$f_G$
$f_0(600)$	$-0.98 \leftrightarrow -0.97$	$0.05 \leftrightarrow 0.07$	$0.20 \leftrightarrow 0.23$	$-0.06 \leftrightarrow -0.08$	$-0.00 \leftrightarrow -0.01$
$f_0(980)$	$-0.05 \leftrightarrow -0.07$	$-0.93 \leftrightarrow -0.90$	$0.11 \leftrightarrow 0.14$	$0.34 \leftrightarrow 0.40$	$\sim -0.02$
$f_0(1370)$	$0.13 \leftrightarrow 0.16$	$-0.25 \leftrightarrow -0.29$	$0.48 \leftrightarrow 0.49$	$-0.83 \leftrightarrow -0.80$	$\sim -0.02$
$f_0(1500)$	$-0.02 \leftrightarrow -0.03$	$-0.03 \leftrightarrow -0.05$	$-0.09 \leftrightarrow -0.10$	$-0.02 \leftrightarrow -0.03$	$\sim -0.99$
$f_0(1710)$	$-0.16 \leftrightarrow -0.19$	$-0.25 \leftrightarrow -0.30$	$-0.85 \leftrightarrow -0.82$	$-0.44 \leftrightarrow -0.43$	$-0.10 \leftrightarrow -0.12$

The fact that the  $f_0(980)$  state considered as the  $f_{NS}$  state mainly has the rather large  $f_{S'}$  component with the sign opposite to the  $f_{NS}$  one suggests a possibility that  $g_{f_0 K\bar{K}}/g_{a_0 K\bar{K}}$  can be about 2, because  $g_{f_0 K\bar{K}}/g_{a_0 K\bar{K}} = |(-AR_{f_0 NS} + A'R_{f_0 N'} + \sqrt{2}A'R_{f_0 S'} + A''R_{f_0 G})/(A \cos\theta_a - A' \sin\theta_a)|$  and  $\theta_a > 0$ . In our model, the  $f_0(1500)$  meson is considered as a glueball, and the  $f_0(1370)$  meson is almost the  $f_{S'}$  state with a rather large  $f_{N'}$  component and the  $f_0(1710)$  meson is almost a  $f_{N'}$  state with a rather large  $f_{S'}$  component.

Because  $g_{f_0 K\bar{K}}$ 's are related to the mixing parameters  $R_{f_0 NS}$ 's and coupling strengths  $A$ ,  $A'$ ,  $A''$  and  $\eta$ - $\eta'$  mixing angle  $\theta_p$ , we executed the best-fit analyses of the various *SPP* decays in the wide range of the  $\lambda_{12}$  value for non-derivative and derivative coupling cases. The best fit-values of  $A$ 's and  $g_{a_0 K\bar{K}}$ 's are tabulated in Tables II and III. These results suggest that the nonderivative coupling seems to be more reasonable than the derivative one and the intermixing parameter  $\lambda_{12}$  is rather large  $0.30 \leftrightarrow 0.35$ .

- |   |   |
|---|---|
| <p>[1] N. N. Achasov and V. N. Ivanchenko, Nucl. Phys. <b>B315</b>, 465 (1989); F. E. Close and N. Isgur, and S. Kumano, Nucl. Phys. <b>B389</b>, 513 (1993); N. N. Achasov and V. V. Gubin, Phys. Rev. D <b>56</b>, 4084 (1997).</p> <p>[2] N. N. Achasov, V. V. Gubin, and V. I. Shevchenko, Phys. Rev. D <b>56</b>, 203 (1997); R. Delbourgo, Dongsheng Liu, and M. D. Scadron, Phys. Lett. B <b>446</b>, 332 (1999); N. N. Achasov, Nucl. Phys. <b>A675</b>, 279c (2000); N. N. Achasov and V. V. Gubin, Phys. Rev. D <b>63</b>, 094007 (2001); A. Gokalop and O. Yilmaz, Phys. Rev. D <b>64</b>, 053017 (2001); N. N. Achasov and A. V. Kiselev, Phys. Rev. D <b>68</b>, 014006 (2003); <b>73</b>, 054029 (2006).</p> <p>[3] D. Black, M. Harada, and J. Schechter, Phys. Rev. D <b>73</b>, 054017 (2006).</p> <p>[4] M. N. Achasov <i>et al.</i> (SND Collaboration), Phys. Lett. B <b>479</b>, 53 (2000); R. R. R. Akhmetshin <i>et al.</i> (CMD-2 Collaboration), Phys. Lett. B <b>462</b>, 371 (1999); <b>462</b>, 380 (1999); A. Aloisio <i>et al.</i> (KLEO Collaboration), Phys. Lett. B <b>536</b>, 209 (2002); <b>537</b>, 21 (2002).</p> <p>[5] W.-M. Yao <i>et al.</i> (Particle Data Group), J. Phys. G <b>33</b>, 1 (2006).</p> | <p>[6] D. Black <i>et al.</i>, Phys. Rev. D <b>59</b>, 074026 (1999); D. Black, A. H. Fariborz, and J. Schechter, Phys. Rev. D <b>61</b>, 074001 (2000).</p> <p>[7] T. Teshima, I. Kitamura, and N. Morisita, J. Phys. G <b>28</b>, 1391 (2002).</p> <p>[8] T. Teshima, I. Kitamura, and N. Morisita, J. Phys. G <b>30</b>, 663 (2004).</p> <p>[9] T. Teshima, I. Kitamura, and N. Morisita, Nucl. Phys. <b>A759</b>, 131 (2005).</p> <p>[10] R. J. Jaffe, Phys. Rev. D <b>15</b>, 267 (1977); M. Alford and R. L. Jaffe, Nucl. Phys. <b>B578</b>, 367 (2000).</p> <p>[11] M. Harada, F. Sannio, and J. Schechter, Phys. Rev. D <b>54</b>, 1991 (1996).</p> <p>[12] D. Aston <i>et al.</i>, Nucl. Phys. <b>B296</b>, 493 (1988).</p> <p>[13] D. V. Bugg, A. V. Sarantsev, and B. S. Zou, Nucl. Phys. <b>B471</b>, 59 (1996).</p> <p>[14] C. Amsler <i>et al.</i>, Eur. Phys. J. C <b>23</b>, 29 (2002); Phys. Lett. B <b>353</b>, 571 (1995); D. Barberis <i>et al.</i>, Phys. Lett. B <b>471</b>, 429 (2000); <b>479</b>, 59 (2000); D. V. Bugg, A. V. Sarantsev, and B. S. Zou, Nucl. Phys. <b>B471</b>, 59 (1996).</p> |
|---|---|